THE APPLICATION OF ACTIVE AND PASSIVE OPTICAL SENSORS IN NATURAL RESOURCE DECISION MAKING

A Paper
Submitted to the Graduate Faculty
of the
North Dakota State University
of Agriculture and Applied Science

By

Donald Vincent Veverka

In Partial Fulfillment of the Requirements
for the Degree of
MASTER OF SCIENCE

Major Program:
Natural Resource Management

November 2020

Fargo, North Dakota

North Dakota State University
Graduate School

Title

THE APPLICATION OF ACTIVE AND PASSIVE OPTICAL SENSORS IN NATURAL RESOURCE DECISION MAKING

By

Donald Vincent Veverka

The Supervisory Committee certifies that this ***disquisition*** complies with North Dakota State University's regulations and meets the accepted standards for the degree of

MASTER OF SCIENCE

SUPERVISORY COMMITTEE:

Dr. Jack Norland
Chair

Dr. Amitava Chatterjee

Dr. Christina Hargiss

Approved:

November 19, 2020
Date

Dr. Edward DeKeyser
Department Chair

ABSTRACT

Remote sensing is becoming a significant tool utilized to study vegetation health and abundance. Vegetation indices (VIs) generated by active and passive remote optical sensors can be implemented in natural resource and agricultural decision-making processes. One such use of vegetation indices is to predict yield and protein contents for various crops. However, the application of VIs is limited due to land use differences and the time period when remote sensing information is most accurate. A literature search was conducted on VIs paying attention to how those are used with sensors mounted on small unmanned aerial vehicles (sUAV). The search found that there was a limited amount of literature being catered towards management decisions compared to scientific studies and systematic reviews. This makes it difficult for decision makers to review and stay updated on remote sensing practices and to incorporate remote sensing into field based management and policy making.

ACKNOWLEDGMENTS

I would like to thank Dr. Jack Norland and Dr. Amitava Chatterjee for the honor of being their graduate student. Dr. Norland has guided me throughout the creation and organization of this master's paper, while Dr. Chatterjee mentored me in all the field applications of this study. Credit must also be given to Dr. Christina Hargiss for being a part of my supervisory committee. Along with, research specialist Norm Cattanach, for providing me with field assistance and agricultural knowledge in pursuit of my degree.

PREFACE

Chapter 1 entitled, “Active and Passive Remote Sensing Application in Natural Resource Decision Making”, describes the background and importance of remote sensing in the environmental decision-making process. Here I discuss the importance of precision agriculture and the application of remote sensing vegetation indices and how they can aid land management decision making.

Chapter 2 entitled, “Comparisons of Sensors to Predict Spring Wheat Grain Yield and Protein Content” is a manuscript I am a co-author on that was submitted to the Agronomy Journal detailing the methodology and results from a field study conducted on 16 sites across the Red River Valley of North Dakota and Minnesota for the 2019 and 2020 growing seasons. Dr. Amitava Chatterjee prepared the document while I was responsible for all the data collection, image processing, and grower communication. Additionally, I contributed to the statistical analysis, writing the methodology, and formatting of the figures and tables represented in the document.

TABLE OF CONTENTS

LIST OF TABLES

LIST OF FIGURES

LIST OF ABBREVIATIONS

ER.....Electromagnetic radiation.

PA.....Precision agriculture.

RENDVI.....Red edge normalized difference vegetation index.

RNDVI .....Red normalized difference vegetation index.

sUAV.....Small unmanned aerial vehicle.

VI .....Vegetation index.

LIST OF APPENDIX TABLES

1. ACTIVE AND PASSIVE REMOTE SENSING APPLICATION IN NATURAL RESOURCE DECISION MAKING

1.1. Literature Review

1.1.1. Importance of precision agriculture

Global farmland (50 million km^2) occupies nearly half of terrestrial land (104 million km^2) (Ritchie and Roser, 2013). A growing population with limited amount of agricultural land, encourages farmers to maximize yield and reduce the environmental impact. An approach to managing resources is through precision agriculture (PA). Precision agriculture is associated with all aspects of agricultural production for the purpose of improving environmental sustainability and crop performance (Radoglou-Grammatikis et al., 2020; Pierce and Nowak, 1999; Shoshany et al., 2013). One aspect of PA is the application of remote sensing technologies and principles to manage spatiotemporal variability of crop health.

Data collection via remote sensing can be achieved by either active or passive optical sensors. Active optical sensors are devices that are designed to produce their own electromagnetic radiation (ER) source and process the reflected optical signature on site instantly (Lamb et al., 2014). Ambient illumination has no impact on active sensors allowing data collection to take place at any time. Passive optical sensors rely on sunlight for an ER source. The reliance on sunlight can introduce more variability and noise in what the passive sensor gathers impacting the quality of data collected. Cloud cover and intermittent ER conditions are just two of the conditions that can introduce variability and noise (Hatfield et al., 2008). These conditions apply to passive sensors designed to be installed on the bottom of small unmanned aircraft vehicles (sUAV).

The application of remote optical sensors can allow farmers to adjust land management practices to increase yield while maintaining sustainability (Weng et al., 2019; Searcy, 1997). Since the 1980s, remote sensing has been used to predict grain yield by collecting satellite data from the National Oceanic and Atmospheric Administration's Advanced Very High-Resolution Radiometer (NOAA-AVHRR) (Bayarjargal et al., 2006; Tucker et al., 1985). In 2003, using the NOAA-AVHRR methodology, red normalized difference vegetation indices (RNDVI) values were used to estimate wheat yields at two different spatial resolutions in North Dakota by inputting the data into an agrometeorological model (Dorainswamy et al., 2003). Measurements were made in late June and early July when the crops were at approximately middle and final vegetative phases of crop development. The model indicated an r^2 value of 0.7 with a root square mean error (RMSE) of 1.11. The higher RMSE is due to the error associated with the satellite's inability to adjust to atmospheric conditions when collecting field data (Dorainswamy et al., 2003). It is vital to reduce the impact of atmospheric conditions to increase the image quality collected by remote sensors. Currently, remote optical sensors have the ability to obtain multispectral banded data and analyze a wider range of VIs with better resolution. Improved resolution can extract more information stored in the image pixels (Nguy-Robertson et al., 2016).

1.1.2. Applying vegetation indices

Analyzed optical sensor data in combination with recorded crop growth stages, can increase crop yield predictability (Becker and Schmidhalter, 2017; Inman et al., 2007). The optical sensor can do this by capturing electromagnetic radiation that is absorbed and reflected depending on the amount of leaf chlorophyll then creating a unique optical reflectance signature (Carlson and Ripley, 1997). Optical signatures can then be transformed to vegetation indices (VIs) like RNDVI. RNDVI is derived as follows:

$$RNDVI = NIR – Red / NIR + Red$$

Where Red is the red wavelength of the ER spectrum centered on 668 nm and NIR is the Near-infrared portion of the spectrum (700-1100nm). This wavelength separates the landscape into water, soil, and vegetation. Live plant leaves only reflect green light while absorbing the blue and red wavelengths. The human eye views a leaf to be green because the pigments of the leaf absorb all other visible wavelengths except for the wavelengths in the green region of the light spectrum. The visible reflection of the green light is a leaf pigment function, while the NIR radiation is reflected by the internal mesophyll structure of the leaf (Khamala, 2017). After passing through the palisade tissue of the leaf and entering the internal leaf cavities, the NIR radiation is either transmitted or reflected. The RNDVI is higher with actively growing vegetation and lower for less actively growing vegetation and non-vegetative factors like soil and water (Khamala, 2017).

The interaction of ER wavelength and leaf function can be detected by the optical sensors and used to generate various VIs via different software. Past field studies and theoretical analyses have portrayed that VIs are related to photosynthetically active radiation and light-dependent physiological processes (Gamon et al., 1995; Glen et al., 2008). Photosynthetic activity can indirectly measure the nitrogen status of crops. Additionally, practical studies have used time-series VIs to measure evapotranspiration (ET) and primary production of vegetation (Glen et al., 2008).

Leaves without stressors like disease and poor water, sunlight, and nutrient availability, absorb blue and red light energy and reflect green light. Therefore, by analyzing a plant's wavelength absorbance and reflectance, remote optical sensors can provide information about crop productivity and health (Khamala, 2017). Generally, a higher RNDVI value indicates

increased chlorophyll content that translates into a more biologically fit crop with an increase in plant size. Chlorophyll has the properties of reflecting green ER, while absorbing the red and blue ER (Blankenship, 2008). Remote optical sensors can detect this biological process to monitor the health status of the crop.

Another VI is the red edge (RE) normalized difference vegetation index (RENDVI). RENDVI is derived as follows:

$$RENDVI = NIR – RE / NIR + RE$$

Where RE is the red edge wavelength of the ER spectrum centered at 717 nm. Similar to RNDVI, the higher RENDVI value can indicate a healthier crop. However, RENDVI uses a narrower band (± 5 nm), hence, the optical signature detects reflectance from further inside the vegetative canopy and data can be collected later in the growing season when the canopy is full (Jorge et al., 2019; Maccioni et al., 2001).

The various VIs that have been developed in remote sensing can successfully monitor crop and soil nutrients, along with, estimating yields with high levels of accuracy (Martin et al., 2012). Two VIs, RNDVI and RENDVI, have been shown to predict spring wheat (*Triticum aestivum* L.) yield (Gopp & Savenkov, 2019; Kouadio et al., 2014; Prey et al., 2018). The estimation of spring wheat yield is vital when establishing agricultural policies, creating regional and national food management plans, and promoting economic sustainability (Tuvdendorj et al., 2019).

Remote optical sensors and VI generation have been widely used for managing crop health and estimation of crop productivity. Numerous factors can contribute to the quality of VIs that impact the yield predictability (Gao et al., 2012). These include rainfall, air temperature, soil characteristics, leaf area, disease, ambient light conditions, growing degree days (GDD), and the

growth stage of the crop. One can take the optical sensor VIs and GDD to determine the crop growth stage that is best used for predicting in-season yield estimations (Raun et al., 2001). In general, the quantitative and qualitative predictability of remote sensor data has a higher level of accuracy of yield prediction with the increase in the GDD throughout the growing season.

Significant relationships between RNDVI and GDD were found using active remote sensing crop sensors for spring wheat yield estimations in North Dakota for the 2012 and 2013 growing seasons (Bu, 2014). The data reported r^2 values ranging from 0.88 to 0.96. Using a regression model, a study done in Mongolia using passive remote sensing from satellites, collected VIs from the years 2000 to 2017 determined that RNDVI (r^2 value of 0.55) was one of the most accurate VIs for predicting yield in spring wheat (Tuvdendorj et al., 2019). Additionally, the results portrayed that the ideal growth stage for yield estimations took place around the flowering stage for spring wheat.

Some of these studies used satellite technology for VI collection, but research has shown that sUAV provide more information in terms of spatial variability (Fernández-Guisuraga et al., 2018) and provided a higher resolution (Iizuka et al., 2018) when collecting vegetation and landscape data. By mounting a passive remote sensor on an aircraft like a sUAV, you alleviate the problems associated with using satellite acquired data. A major satellite problem is the inability to account for the current atmospheric conditions for the desired field area (Mkhabela et al., 2011). Fog and excessive cloud cover can reduce the image quality captured by the sensor that can decrease the accuracy of VI generation. Therefore, by attaching a passive optical sensor to a sUAV, one can initiate a pre-set flight plan at the ideal time frame when the atmospheric conditions are optimal (Mulla, 2013). The VIs produced with sensor readings from a sUAV can increase accuracy and precision, giving the producer the best available advice to improve yield.

Exposed soil and low canopy cover create a low biochemical signal making it difficult for remote sensors to record VIs. A study conducted in Yellowstone National Park (Mirik et al., 2005) looked at the potential of a hyperspectral 1-m remote sensor's ability to reduce the time spent and spatial errors with traditional forage nutrient analysis. After analyzing data from a wide range of vegetative communities, they found there were no strong linear relationships (r^2 <0.3) between a variety of VIs and nitrogen, phosphorous, and neutral detergent fibers on a dry matter basis ($g*g^{-1}$ x 100). The primary reason why this study exhibited a lack of relationship is due to the presence of excessive non-photosynthetic vegetation like bark, stems, and litter along with bare ground. However, a similar remote sensing study conducted by the same researchers (Mirik et al., 2005) in the same location, found significant results when analyzing RNDVI from the hyperspectral data and regressed against ground-collected biomass. Results indicated a strong relationship when collecting VIs from sedge, willow, and total biomass (r^2>0.66). However, weak relationships were found between grass, forb, and litter biomass (r^2<0.51). Similarly, the weak relationships were because of the presence of branch and twig materials that interfere with the spectral signal from the vegetation to the sensor. Therefore, VIs can be a useful tool to make land management decisions if the canopy cover for crops and other vegetation exceed that of the exposed soil and non-photosynthetic material.

1.1.3. How decision makers can utilize remote sensing information

The National Research Council (2007) states that with a growing population and heightened concerns for human health and global food security, the application of remote sensing technology can be utilized to aid in the decision-making process in a more efficient manner (National Research Council, & Geographical Sciences Committee, 2007). As discussed before, the understanding that leaf reflectance changes with the physical and chemical characteristics of

the plant, along with the ability to detect emitted wavelengths and generate VIs, remote optical sensors can be a tool for nutrient status and yield predictions. Individuals such as, environmental consultants, land management specialists, and producers can identify and utilize these results for implementation into their environmental decision-making process (Hatfield et al., 2008).

Both active and passive sensors have been known to provide similar VI readings. Previous studies found a close relationship between RNDVI collected by active and passive optical sensors (Erdle, et al., 2011; Fitzgerald, 2010; Gozdowski et al., 2020). Active optical sensors have been found to measure green cover with roughly the same amount of accuracy as passive optical sensors (Fitzgerald, 2010). Additionally, researchers found no difference in the performance of passive aerial sensors and ground-based active sensors (Krienke et al., 2017). Moreover, (Schut et al., 2018) found that spatial variability in sUAV derived VI values at the plot scale was significantly related to differences in yields and fertilizer responses.

Since passive optical sensors can be mounted to a sUAV they can collect data over a greater surface area compared to handheld active sensors. Passive sensors are also less labor intensive because they can be flown automatically with the desired resolution and perimeter to cover. Active sensors require walking over larger areas while collecting a smaller amount of data. Not only is that method inefficient for large scale management, active sensor operation can increase disturbance to the land. Although passive sensors have the ability to cover a larger area more efficiently, the quality of data is dependent on the ambient light conditions. Ideally, if the technology for active optical sensors advances to be able to detect wavelengths from a greater distance, then those sensors can be mounted on sUAVs and be deployed at any time of day. Eliminating the ambient light factor can allow for more frequent data collection.

The use of scientific evidence is widely shared among public and private institutions, but it has yet to be utilized widely in environmental policy and decision making (Sutherland et al., 2004; Matzek et al., 2014; Cook et al., 2012; Dicks et al., 2014). When investigating if this lack of utilization in decision making applies to VIs from sUAV and active sensors, I proposed to survey the literature for applications in decision making. Out of all the research publications I reviewed it was estimated that 1 out of every 8 articles (approximately 50 total articles reviewed) about remote sensing had applicable information related to sUAVs and active sensors. This is less compared to the amount of satellite based remote sensing research (Lobell et al., 2003; Wu et al., 2015). I think if there is a greater push for sUAV based remote sensing information published in scientific journals with a focus on decision making, then we could see more sUAVs being utilized by decision makers. This is being accomplished to a certain extent by some universities in the United States which have extension publications related to sUAV applications (Adamchuk et al., 2020; Buckland et al., 2020; Purdue Extension, 2020). Still the lack of scientific journals publishing and requiring more focus on decision making is needed for the full utilization of VIs and sUAVs.

My review of scientific literature found that communicating the use of VIs with sUAVs is a practical and efficient method should be more abundant than what it is. I believe this issue stems from a communication barrier between researchers and other environmental professionals specializing in PA. Not in the transfer of information, but in the writing objectives and style (Dicks et al., 2014). Most scientific publications are written to be circulated within academia and utilized by fellow researchers, making it difficult for decision makers to review and incorporate sUAV based remote sensing results into the decision-making process. The burden for decision makers and those that advise them of staying updated on research literature when it is not written

to incorporate new knowledge into decision making needs to be continually addressed. Whether it is field based management or policy making, an increase in research and extension literature catered toward decision makers on the uses of sUAV remote sensing and applications of optical sensors can result in more environmentally and economically sustainable practices to manage our natural resources.

1.2. Future Considerations

Active and passive optical sensors manufactured for the agriculture industry will be utilized more frequently in the coming years. The positive relationships between the active and passive VI data collection and the effectiveness of yield predictability supports the increased implementation of remote sensing in agriculture production. As the technology improves, I foresee a future where sUAV can further minimize abiotic limitations or develop an active aerial sensor to eliminate ambient light dependence. The implementation of sUAV remote sensing can be a practical solution to aid in increasing crop yields while improving ecosystem health.

1.3. References

Adamchuk, V., Perk, R., & Schepers, J. (2020). Applications of Remote Sensing in Site-Specific Management. University of Nebraska Cooperative Extension, University of Nebraska, EC 03-702

Bayarjargal, Y., Karnieli, A., Bayasgalan, M., Khudulmur, S., Gandush, C., & Tucker, C. J. (2006). A comparative study of NOAA–AVHRR derived drought indices using change vector analysis. *Remote Sensing of Environment*, *105*(1), 9-22.

Becker, E., & Schmidhalter, U. (2017). Evaluation of yield and drought using active and passive spectral sensing systems at the reproductive stage in wheat. *Frontiers in plant science*, 8, 379.

Benedetti, R., & Rossini, P. (1993). On the use of NDVI profiles as a tool for agricultural statistics: the case study of wheat yield estimate and forecast in Emilia Romagna. *Remote Sensing of Environment*, *45*(3), 311-326.

Blankenship, R. E. (2008). Molecular mechanisms of photosynthesis. *Molecular Mechanisms of Photosynthesis*.

Bu, H. (2014). Yield and quality prediction using satellite passive imagery and ground-based active optical sensors in sugar beet, spring wheat, corn, and sunflower (Doctoral dissertation, North Dakota State University).

Buckland, K., Rasmussen, A., & Nackley, L. (2020). Unmanned Aerial Systems: A guide for finding the right system for your Oregon farm. OSU Extension Catalog, Oregon State University, EM 9298

Carlson, T. C., & Ripley, D. A. (1997). On the relationship between NDVI, fractional vegetation cover and leaf area index. *Remote Sensing of the Environment*. 62:241-252.

Cook, C. N., Carter, R. B., Fuller, R. A., & Hockings, M. (2012). Managers consider multiple lines of evidence important for biodiversity management decisions. *Journal of Environmental Management*, *113*, 341-346.

Dicks, L. V., Walsh, J. C., & Sutherland, W. J. (2014). Organising evidence for environmental management decisions: a '4S'hierarchy. *Trends in ecology & evolution*, *29*(11), 607-613.

Doraiswamy, P. C., Moulin, S., Cook, P. W., & Stern, A. (2003). Crop yield assessment from remote sensing. *Photogrammetric engineering & remote sensing*, 69(6), 665-674.

Erdle, K., Mistele, B., & Schmidhalter, U. (2011). Comparison of active and passive spectral sensors in discriminating biomass parameters and nitrogen status in wheat cultivars. *Field Crops Research*, 124(1), 74-84.

Extension.purdue.edu. (2020). *Purdue Extension*. [online] Available at: <https://extension.purdue.edu/> [Accessed 4 November 2020].

FAOSTAT. FAO. Statistical Yearbooks—World food and agriculture. Food Agric. *Organizat. United Nations* 2013, 288 pp (2014).

Fernández-Guisuraga, J. M., Sanz-Ablanedo, E., Suárez-Seoane, S., & Calvo, L. (2018). Using unmanned aerial vehicles in postfire vegetation survey campaigns through large and heterogeneous areas: Opportunities and challenges. *Sensors*, 18(2), 586.

Fitzgerald, G. J. (2010). Characterizing vegetation indices derived from active and passive sensors. *International Journal of Remote Sensing*, 31(16), 4335-4348.

Gamon, J. A., Field, C. B., Goulden, M. L., Griffin, K. L., Hartley, A. E., Joel, G., ... & Valentini, R. (1995). Relationships between NDVI, canopy structure, and photosynthesis in three Californian vegetation types. *Ecological Applications*, *5*(1), 28-41.

Gao, Y., Huang, J., Li, S., & Li, S. (2012). Spatial pattern of non-stationarity and scale-dependent relationships between NDVI and climatic factors—A case study in Qinghai-Tibet Plateau, China. *Ecological Indicators*, *20*, 170-176.

Glenn, E. P., Huete, A. R., Nagler, P. L., & Nelson, S. G. (2008). Relationship between remotely-sensed vegetation indices, canopy attributes and plant physiological processes: What vegetation indices can and cannot tell us about the landscape. *Sensors*, 8(4), 2136-2160.

Gopp, N. V., & Savenkov, O. A. (2019). Relationships between the NDVI, Yield of Spring Wheat, and Properties of the Plow Horizon of Eluviated Clay-Illuvial Chernozems and Dark Gray Soils. *Eurasian Soil Science*, *52*(3), 339-347.

Gozdowski, D., Stępień, M., Panek, E., Varghese, J., Bodecka, E., Rozbicki, J., & Samborski, S. 232 (2020). Comparison of winter wheat NDVI data derived from Landsat 8 and active optical sensor at field scale. *Remote Sensing Applications: Society and Environment*, 20, 100409.

Hannah Ritchie and Max Roser (2013) - "Land Use". Published online at OurWorldInData.org. Retrieved from: 'https://ourworldindata.org/land-use' [Online Resource]

Hatfield, J. L., Gitelson, A. A., Schepers, J. S., &Walthall, C. L. (2008). Application of spectral remote sensing for agronomic decisions. *Agronomy Journal*.

Iizuka, K., Itoh, M., Shiodera, S., Matsubara, T., Dohar, M., & Watanabe, K. (2018). Advantages of unmanned aerial vehicle (UAV) photogrammetry for landscape analysis compared with satellite data: A case study of postmining sites in Indonesia. *Cogent Geoscience*, 4(1), 1498180.

Jorge, J., Vallbé, M., & Soler, J. A. (2019). Detection of irrigation inhomogeneities in an olive grove using the NDRE vegetation index obtained from UAV images. *European Journal of Remote Sensing*, 52(1), 169-177.

Khamala, E. (2017). Review of the available remote sensing tools, products, methodologies and data to improve crop production forecasts. Food and Agriculture Organization of the United Nations (FAO).

Kouadio, L., Newlands, N. K., Davidson, A., Zhang, Y., & Chipanshi, A. (2014). Assessing the performance of MODIS NDVI and EVI for seasonal crop yield forecasting at the ecodistrict scale. *Remote Sensing*, *6*(10), 10193-10214.

Krienke, B., Ferguson, R. B., Schlemmer, M., Holland, K., Marx, D., & Eskridge, K. (2017). Using an unmanned aerial vehicle to evaluate nitrogen variability and height effect with an active crop canopy sensor. *Precision Agriculture*, 18(6), 900-915.

Lamb, D. W., Schneider, D. A., & Stanley, J. N. (2014). Combination active optical and passive thermal infrared sensor for low -level airborne crop sensing. *Precision Agriculture*, 15(5): 523-521.

Lobell, D. B., Asner, G. P., Ortiz-Monasterio, J. I., & Benning, T. L. (2003). Remote sensing of regional crop production in the Yaqui Valley, Mexico: estimates and uncertainties. *Agriculture, Ecosystems & Environment*, *94*(2), 205-220.

Maccioni, A., Agati, G., & Mazzinghi, P. (2001). New vegetation indices for remote measurement of chlorophylls based on leaf directional reflectance spectra. Journal of Photochemistry and Photobiology B: *Biology*, 61(1-2), 52-61.

Martin, K., Raun, W., & Solie, J. (2012). By-plant prediction of corn grain yield using optical sensor readings and measured plant height. *Journal of Plant Nutrition*, 35(9): 1429-1439.

Matzek, V., Covino, J., Funk, J. L., & Saunders, M. (2014). Closing the knowing–doing gap in invasive plant management: accessibility and interdisciplinarity of scientific research. *Conservation Letters*, *7*(3), 208-215.

McNie, E. C. (2007). Reconciling the supply of scientific information with user demands: an analysis of the problem and review of the literature. *Environmental science & policy*, *10*(1), 17-38.

Mkhabela, M. S., Bullock, P., Raj, S., Wang, S., & Yang, Y. (2011). Crop yield forecasting on the Canadian Prairies using MODIS NDVI data. *Agricultural and Forest Meteorology* 151(3), 383-393.

Mulla, D. J. (2013). Twenty five years of remote sensing in precision agriculture: Key advances and remaining knowledge gaps [Special Issue]. *Biosystems Engineering* 114, 358-371.

National Research Council, & Geographical Sciences Committee. (2007). *Contributions of Land Remote Sensing for Decisions about Food Security and Human Health: Workshop Report*. National Academies Press.

Nguy-Robertson, A., Brinley-Buckley, E., Suyker, A., Awada, T. N. (2016). Determining factors that impact the calibration of consumer-grade digital cameras used for vegetation analysis. *International Journal of Remote Sensing*, 37(14), 3365-3383.

Pierce, F. J., & Nowak, P. (1999). Aspects of precision agriculture. In Advances in agronomy (Vol. 67, pp. 1-85). Academic Press.

Prey, L., Von Bloh, M., & Schmidhalter, U. (2018). Evaluating RGB imaging and multispectral active and hyperspectral passive sensing for assessing early plant vigor in winter wheat. *Sensors*, 18(9), 2931.

Radoglou-Grammatikis, P., Sarigiannidis, P., Lagkas, T., & Moscholios, I. (2020). A compilation of UAV applications for precision agriculture. *Computer Networks*, *172*, 107148.

Research and markets. (2018). Global Agriculture Drone Market Analysis & Trends – Industry Forecast to 2027.

Schut, A. G. T., Traore, P. C. S., Blaes, X., & de By, R. A. (2018). Assessing yield and fertilizer response in heterogeneous smallholder fields with UAVs and satellites. *Field Crops Research*, 221, 98-107.

Searcy, S. W. (1997). Precision farming: A new approach to crop management (Publication No. L-5177). College Station, TX: Texas Agriculture Extension Service.

Shoshany, M., Long, D., & Bonfil, D. (2013). Remote Sensing for sustainable agriculture. *International Journal of Remote Sensing*, 34(17), 6021-6023.

Sutherland, W. J., Pullin, A. S., Dolman, P. M., & Knight, T. M. (2004). The need for evidence-based conservation. *Trends in ecology & evolution*, *19*(6), 305-308.

Tucker, C. J., Townshend, J. R., & Goff, T. E. (1985). African land-cover classification using satellite data. *Science*, 227(4685), 369-375.

Tuvdendorj, B., Wu, B., Zeng, H., Batdelger, G., & Nanzad, L. (2019). Determination of Appropriate Remote Sensing Indices for Spring Wheat Yield Estimation in Mongolia. *Remote Sensing*, 11(21), 2568.

Weng, Q., Gamba, P., Chen, K. S., & Wang, G. (2019). Foreword Remote Sensing for Environmental Sustainability in the Asian─ Pacific Region. *IJSTA*, *12*(11), 4172-4174.

Wu, B., Gommes, R., Zhang, M., Zeng, H., Yan, N., Zou, W., ... & Van Heijden, A. (2015). Global crop monitoring: a satellite-based hierarchical approach. *Remote Sensing*, *7*(4), 3907-3933.

2. COMPARISONS OF SENSORS TO PREDICT SPRING WHEAT GRAIN YIELD AND PROTEIN CONTENT[1]

2.1. Abstract

Mapping of canopy vegetation indices can provide a spatial variability in grain yield before harvest. Canopy reflectance data from a hand-held active sensor (RapidScan CS-45) and a small unmanned aerial vehicle (sUAV)-based passive light optical sensor (Micasense RedEdge) were compared based on vegetation indices (VIs), red normalized vegetation (RNDVI) and red edge normalized vegetation (RENDVI). Potential of VIs to predict spring wheat (*Triticum aestivum* L.) grain yield and protein content were examined for data from 16 site-years in the Red River Valley of Minnesota and North Dakota. At each site, reflectance data were collected three times during June and July. Linear regression between two sensors showed a significant ($p<0.05$) relationship based on RNDVI (0.69) and RENDVI (0.55) values ($n=48$). At Feeks growth stages>12 RENDVI from both sensors could predict the grain yield; but only the RENDVI from sUAV-based passive sensor could predict the protein content at Feekes stages between five and eight. Use of sUAV based passive sensor has potential to predict grain yield and protein content but selecting the growth stage for collecting reflectance data is critical for the accurate prediction.

[1]The material in this chapter was co-authored by Donald Veverka and Dr. Amitava Chatterjee. Donald Veverka had primary responsibility for collecting data in the field and for processing all raw imagery into generated VIs with supporting figures. Donald Veverka was the primary developer of the materials and methods that are advanced here. Donald Veverka also drafted and revised all versions of this chapter to fit the format as directed by the NDSU graduate school. Dr. Amitava Chatterjee served as proofreader and checked the math in the statistical analysis conducted by Donald Veverka.

2.2. Introduction

Predicting the spatial variability in crop yield and quality before harvest is critical for precision farming (Marino & Alvino, 2020). Growers are interested in methods for estimating wheat grain yield and protein content at earlier growth stages (Goodwin et al., 2018). Remote sensing-based indices like red normalized vegetation index (RNDVI) and red edge normalized vegetation index (RENDVI) are sensitive to biomass and nitrogen (N) variability in crop canopies (Naser et al., 2020). Since the mid-1990s, orthomosaic images of canopy reflectance have been extensively used in making decisions for crop and nutrient management (Roberts et al., 2012; Sripada et al., 2006). Canopy reflectance data can be collected using active and passive sensors. Passive sensors depend on the sunlight whereas active sensors use an internal light source. Passive sensors require calibration and data processing techniques to rectify for sun angle, illumination, camera optics, rectification of imagery and require specialized software to analyze the imagery (Krienke et al., 2017). On-the-go active optical crop canopy sensors, such as GreenSeeker (Trimble Navigation Limited, Sunnyvale, California, USA), Crop Circle, RapidScan (Holland Scientific Inc., Lincoln, Nebraska, USA) were extensively used to overcome the limitation of passive sensing devices and to minimize the effect of ambient light conditions on reflectance readings (Li et al., 2014; Tubana et al., 2011). However, currently available active sensors require close proximity to the target due to the light source intensity. Integration of sensor technologies, small unmanned aerial vehicle (sUAV), and image processing software have demonstrated their versatility and cost-benefits across a wide range of applications (Bendig et al., 2015; Kyratzis et al., 2017; Maimaitijiang et al., 2020). This study aims at comparing active (handheld) and passive (VIs derived by UAV imagery) sensors based on

RNDVI and RENDVI indices across spring wheat growers' fields in the Red River Valley (RRV) of Minnesota and North Dakota.

One important limitation to the widespread use of remote sensing tools is the lack of algorithms that would be reliable in a variety of soil and weather conditions (Bean et al., 2018; Samborski, et al., 2009). Bean et al. (2018) reported that active optical reflectance has been successful in generating fertilizer N demand to optimize N use efficiency in some fields, but locally derived algorithms have not been validated outside the region within which they were developed. Major challenges in developing algorithms are the selection of growth stages for monitoring canopy reflectance, and VIs suitable for the prediction at large spatial scale (Zhou et al., 2017). Several researchers (Bendig et al., 2015; Sharma et at., 2015) reported that visible band VIs work for early growing stages only. Within the red wavelength, green leaves have a reflectance of 20% or less in the 500-700 nm range; but the red edge and infrared wavelengths reflect as high as 60% in the 700 to 1300 nm range (Sharma et al., 2015). Further, (Aparicio et at., 2000) found that the best correlation between vegetation indices like RNDVI and yield was achieved at anthesis; but in the irrigated environment, the significant relationship between IS and yield was restricted to later stages of durum winter wheat (*Triticum turgidum* L.). Kryatzis et al. (2017) found both positive and negative correlations between yield and canopy reflectance during grain filling of durum wheat, indicating that environmental conditions at grain filling could affect the relationship.

Before wide application of precision tools, we should validate the relationship between active and passive sensors across large spatial scale. Spring wheat occupies a significant agricultural land in the RRV of North Dakota and Minnesota. It is critical to identify ideal growth stages to develop algorithms for spring wheat grain yield and protein content prediction

using active and passive sensors. Main objectives of this study were to (i) determine the relationships of VIs determined by active and passive sensors, (ii) determine changes in VIs over growing seasons, (iii) develop algorithms to predict grain yield and protein content using VIs from active and passive sensors, and (iv) identify growth stage(s) suitable for yield and protein prediction.

2.3. Materials and Methods

Canopy reflectance data were collected from sixteen spring wheat growers' fields located across the Red River Valley of Minnesota and North Dakota during 2019 and 2020 growing seasons (eight sites each year). Location, spring wheat cultivar, previous crop and fertilizer N application rate of these fields are presented in Table 1. More detailed site and crop management information are presented in Appendix Table 1. All fields are conventionally tilled. After growers planted their field, a representative plot area, 30 m long and 15 m wide, was established for making reflectance measurements. Canopy reflectance data was collected using a handheld active light optical sensor (RapidSCAN CS-45, Holland Scientific Inc., Lincoln, NE) and a passive light optical sensor, MicaSense RedEdge (Micasense Inc., Seattle, WA) attached to a sUAV, DJI Matrice 100 (DJI, Shen Zhen, China). For both years, three observations of canopy reflectance were collected using both sensors (on the same day) during June and July (Appendix Table 2).

Table 1. Geographic location, spring wheat cultivar, previous crop, grain yield and protein concentration of sixteen growers' fields (NA: not available)

Site	Location	Cultivar	Previous Crop	Fertilizer-N	Grain Yield	Protein
				kg N ha^{-1}	Mg ha^{-1}	g kg^{-1}
2019						
Argyle, MN	48°18'22.6"N 96°56'12.4"W	Westbred9590	Soybean	157	1.66	162
Gentilly, MN	47°47'9.51"N 96°56'45.0"W	Westbred9590	Soybean	162	1.42	133
Dorothy, MN	47°55'14.1"N 96°29'43.3"W	Linkert	Soybean	151	2.95	149
Mahnomen, MN	47°30'31.2"N 95°53'56.2"W	Trigger	Soybean	168	2.83	106
Ada, MN	47°23'44.5"N 96°41'3.12"W	Shelly	Soybean	179	1.53	157
Red lake Falls, MN	47°49'53.2"N 96°14'47.1"W	Ingmar	Soybean	134	1.66	158
Thief River Falls, MN	48°2'3.82"N 96°14'38.9"W	Valda	Soybean	100	1.91	124
Rustad, MN	46°43'13.4"N 96°41'51.6"W	Bollers	Soybean	123	1.59	168
2020						
Argyle, MN	46°36'25.2"N 96°36'55.4"W	Westbred9479	Soybean	184	4.72	147
Gentilly, MN	47°46'44.0"N 96°27'30.9"W	Westbred9590	Soybean	175	4.86	122
Ada_GM, MN	47°21'10.6"N 96°25'10.5"W	AgriPro	Soybean	169	5.82	153
Ada, MN	46°15'12.3"N 96°27'30.2"W	Valda	Spring Wheat	142	2.87	157
Fosston, MN	47°30'40.8"N 95°48'39.6"W	Rebel	Sugarbeet	134	5.26	160
Casselton, ND	46°52'38.2"N 97°15'15.1"W	NA	NA	NA	6.65	133
Rustad-no tile, MN	46°43'4.5"N 96°42'7.92"W	Prosper	Sugarbeet	190	10.6	179
Rustad-Tile, MN	46°36'25.2"N 96°36'55.4"W	Lang	Sugarbeet	168	7.59	180

Observation dates for three sets of readings were different across sites; because of time limitation, as passive sensor readings need to be collected around solar noon, and long travelling duration between sites. During 2019, 1st, 2nd, and 3rd set of readings were collected during Jun 18, 19 and Jun 26, July 12 and July 16, and July 22nd and 23rd, respectively. Next year, 1st, 2nd, and 3rd readings were collected on June 5, 11, and 12, June 19, 22 and 22, and July 10, 15 and 16, respectively. First set of readings corresponds to Feekes growth stages 5-9, and 2nd and 3rd readings were taken at stages>12.

The active sensor has an internal GPS and a polychromatic light source with spectral bands, 670 nm, 730 nm and 780 nm. Canopy reflectance data was collected by walking at a constant pace and held at a constant height and data was downloaded by RapidTALK software (Holland Scientific Inc., Lincoln, Nebraska, USA). The passive optical sensor measures five wavelengths, blue (475 nm), green (560 nm), red (668 97 nm), near infrared or NIR (840 nm) and red edge (717 nm). The sUAS was flown at a constant elevation of 91 m at a speed of 8 m s^{-1}, with 80% side and frontal image overlap. Before and after the flight for each observation day, calibrated reflectance panel image was taken to adjust light conditions during flight. The sUAV flight was maneuvered using DJI Ground Station Pro applications on an Ipad Mini (Apple, Cupertino, CA). Images were collected during solar noon, between 10.00 and 14.00 h, to ensure consistent light conditions. Raw pixel values of orthomosaic images were transformed to absolute spectral radiance values provided by Micasense. Spectral radiance values of the plot area were analyzed using Pix4D software (Pix4D, Lausanne, Switzerland).

Vegetation indices RNDVI and RENDVI of active and passive sensors were calculated using the following equations.

$$RNDVI = (NIR - Red)/(NIR + Red)$$

$$RENDVI = (NIR - Red\ edge)/(NIR + Red\ edge)$$

At maturity, grain yield was determined by hand harvesting four representative subplots of 9 m by 0.3 m. Grain moisture and protein content were determined using near infrared analyzer.

2.4. Statistical Analysis

Exploratory statistical analyses of soil properties applied fertilizer-N, grain yield and protein content were studied across eight sites during 2019-2020 growing seasons. Relationships between active and passive sensors were determined for vegetation indices, RNDVI and

RENDVI using linear regression curve fit at 95% significance level using SAS Enterprise Guide 7.1 (SAS Institute Inc., Cary NC). Linear regression coefficients and significance of the model between vegetation indices of active and passive sensors and grain yield and protein content were determined for three observation dates of two growing seasons.

2.5. Results and Discussion

2.5.1. Site and growing season condition

Monthly rainfall and average temperature data of all sites were collected from the nearest North Dakota Agriculture Weather Network stations (https://ndawn.ndsu.nodak.edu/) are presented in Appendix Table 2. Both growing seasons have early dry condition and extreme wet during late growing season. Most sites have a medium-textured soil except for the Casselton site in 2020 (Appendix Table 1). Soils are neutral to alkaline with organic matter content. Initial available phosphorus and potassium had a wide range from very low (16 g kg^{-1}), and low (41-80 g kg^{-1}) to very high (>151 g kg^{-1}). In most cases, soybean was previous crop and growers used a wide range of cultivars. Amount of fertilizer-N ranged between 100-190 kg N ha^{-1} with a mean value of 150 kg N ha^{-1}. Wheat was planted in between April 21 to May 15 and harvested within Aug. 12 for both seasons (Appendix Table 1). In 2020, average grain yield and protein concentration of 5.96 Mg ha^{-1}, 157 g kg^{-1}, respectively, were higher than respective values (1.94 Mg ha^{-1}, 145 g kg^{-1}, respectively) in 2019 growing season (Table 1).

2.5.2. Relationship between active and passive sensors

Considering readings collected at three observation dates from sixteen sites during 2019 and 2020 (n=48), RNDVI and RENDVI readings of passive sensor had a significant relationship with active sensor (Fig. 1). Passive sensor can explain 69% and 55% of variability in RNDVI and RENDVI readings of active sensor with error values of 5% and 7%, respectively. According

to the slope value of linear fit, passive sensor underestimate RNDVI values and overestimate RENDVI values. Previous studies (Erdle et al., 2011; Fitzgerald, 2010; Gozdowski et al., 2020) also found a close relationship between RNDVI collected by active and passive sensors. (Schut et al., 2018)) found that spatial variability in sUAV derived VI values at the plot scale was significantly related to differences in yields and fertilizer responses. Fitzgerald (2010) found that active sensor appears to be able to measure green cover with about the same accuracy as passive sensors. Erdle et al. (2011) observed testing and comparing one bi-directional hyperspectral passive sensor and three active sensors, the shoot biomass and N status wheat could well be estimated across two growing seasons. Researchers also found no difference in the ability of aerial and ground-based active sensors (Krienke et al., 2017). Godzowski et al. (2020) reported that a linear model might be adequate to describe the relationship between ground and satellite-based RNDVI; but it was difficult to obtain a perfect 1:1 relationship due to differences in wavelengths of Red and NIR reflectance, and dates of data acquisition.

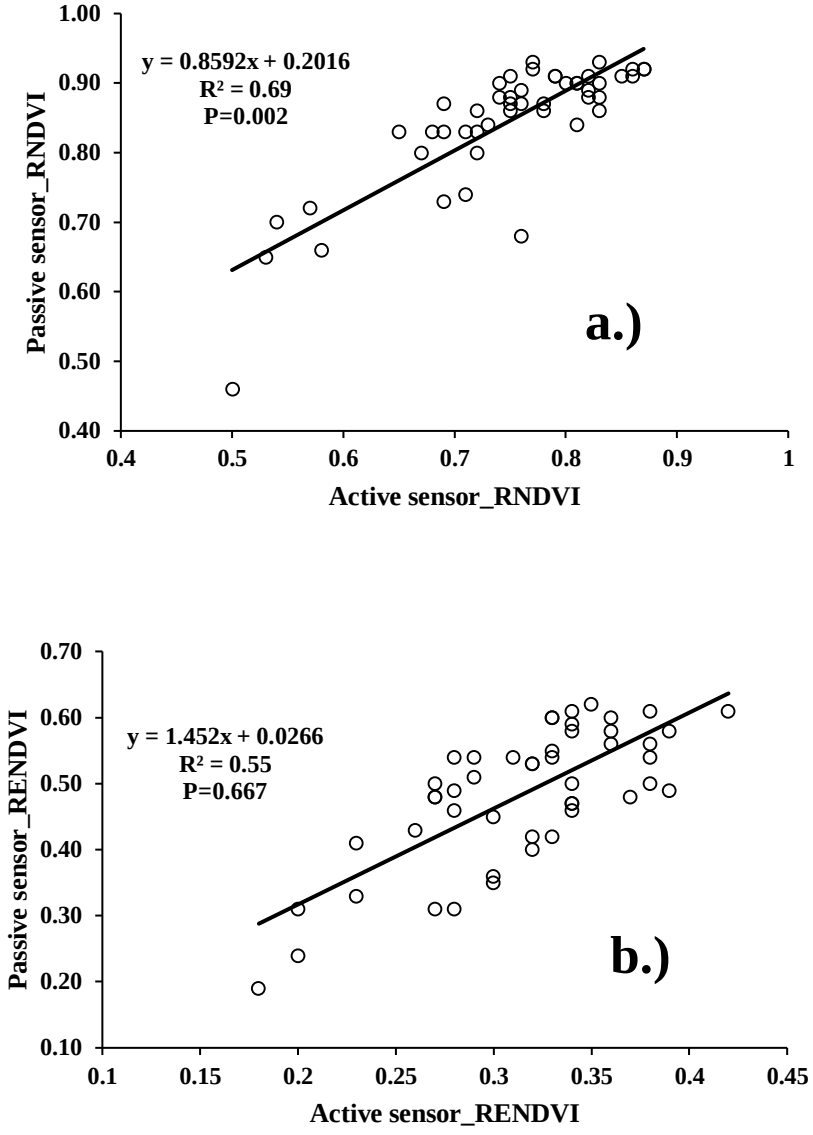

Figure 1. Linear regression fit of vegetation indices, (a) RNDVI and (b) RENDVI data collected using handheld active and sUAV based passive sensors from sixteen spring wheat fields during 2019 and 2020 growing seasons

2.5.3. Prediction of grain yield

Changes in RNDVI and RENDVI from active and passive sensors for three observations across sixteen sites during 2019 and 2020 are presented in Appendix Table 3. Both, RNDVI and RENDVI readings of both sensors dropped from 1st to 3rd observation date. The decrease in RNDVI at the end of the season was attributed to leaf senescence and physiological maturity which increased red band reflectance and decreased NIR band reflectance (Naser et al. 2020). Linear regression coefficient (r^2) and p value of F statistics, for the relationships between grain yield and protein concentration with vegetation indices from active and passive sensors' reflectance data, are presented in Table 2. Grain yield showed a significant linear relationship with the third set of RENDVI readings i.e., at Feekes stages>12 of both sensors for both years.

For the rice grain yield prediction, Zhou et al. (2017) found that VIs composed of red edge band (720 mm) and near infrared band (800 mm) were effective. It is important to note that active sensor has higher r^2 value than passive sensor in 2019; but the opposite trend was observed in 2020. Better performance of RENDVI over RNDVI in yield prediction particularly at late growth stages was also observed by several researchers (Bendig et al., 2015; Guan et al., 2019; Sharma et al., 2015). Bendig et al. (2015) concluded that visible band VIs work only for early growing stages only. Ability and accuracy of wheat grain yield prediction increased as the growing season progressed from Feekes 3 to 10 stages for a 22 site-years of N fertility trials (Bushong et al., 2016). Values of RNDVI were highly correlated to yield (r^2= 0.601- 0.809) from the middle reproductive to early ripening stage (Guan et al., 2019). Naser et al. 174 (2020) reported RNDVI showed significant relationship with yield at the anthesis and mid-grain filling growth stages only, when the sensor is not saturated i.e., NDVI. In this study, RNDVI values are

Table 2. Regression coefficient among vegetation indices (RNDVI and RENDVI) measured by passive (Micasense) and active (RapidScan) sensors at three different growth stages during growing seasons (Flight 1-Tillering, Flight 2-Stem Extension, Flight 3-Heading) and wheat grain yield and protein at 16 sites in the Red River Valley of ND and MN during 2019 and 2020 growing seasons (Bold values indicate significant relationship at 95% significance level)

Year	Sensor	Indices	Readings	Grain yield (Mg ha^{-1})			Protein (g kg^{-1})		
				Model	r^2	Pr>F	Model	r^2	Pr>F
2019	Micasense	RNDVI	1st		0.01	0.79		0.08	0.49
			2nd		0.03	0.66		0.09	0.45
			3rd		0.43	0.07		0.39	0.09
		RENDVI	1st		0.26	0.20	342x-19.1	**0.60**	**0.02**
			2nd		0.01	0.77		0.05	0.60
			3rd	11.2x-3.89	**0.55**	**0.03**		0.21	0.25
	RapidScan	RNDVI	1st		0.01	0.79		0.11	0.42
			2nd		0.03	0.65		0.12	0.40
			3rd		0.21	0.25		0.23	0.22
		RENDVI	1st		0.01	0.98		0.21	0.25
			2nd		0.01	0.82		0.21	0.25
			3rd	22.1x-4.53	**0.69**	**0.01**		0.35	0.12
2020	Micasense	RNDVI	1st		0.18	0.29		0.43	0.07
			2nd		0.04	0.63		0.41	0.08
			3rd		0.46	0.06		0.02	0.72
		RENDVI	1st		0.28	0.17	162x+99.9	**0.51**	**0.04**
			2nd		0.12	0.40	169x+66.6	**0.61**	**0.02**
			3rd	-21.4x+15.9	**0.63**	**0.01**		0.08	0.50

Table 2. Regression coefficient among vegetation indices (RNDVI and RENDVI) measured by passive (Micasense) and active (RapidScan) sensors at three different growth stages during growing seasons (Flight 1-Tillering, Flight 2-Stem Extension, Flight 3-Heading) and wheat grain yield and protein at 16 sites in the Red River Valley of ND and MN during 2019 and 2020 growing seasons (Bold values indicate significant relationship at 95% significance level) (continued)

Year	Sensor	Indices	Readings	Grain yield (Mg ha^{-1})			Protein (g kg^{-1})		
				Model	r^2	Pr>F	Model	r^2	Pr>F
	RapidScan	RNDVI	1st		0.06	0.55		0.13	0.38
			2nd		0.11	0.42		0.01	0.97
			3rd		0.40	0.09		0.02	0.75
		RENDVI	1st		0.11	0.42		0.25	0.20
			2nd		0.01	0.86		0.25	0.21
			3rd	-37.2x+16.2	**0.51**	**0.04**		0.06	0.53

close to 0.8-0.9 since our 1st reading. Once leaves completely cover the row, RNDVI readings fall into narrow range, making it difficult to yield predictions (Sharma et al., 2015)

2.5.4. Prediction of grain protein concentration

For both seasons, RENDVI of sUAV based passive sensor was significantly correlated with protein during first observation. In 2020, second observation of RENDVI using passive sensor was also correlated to protein content (Table 2). This study was comprised of 12 cultivars with protein concentration ranging between 106 to 180 g kg^{-1} (Table 1). For both years, the highest r^2 value was close to 0.6, indicating it can explain approximately 60% variation in protein content. Grain protein content is a product of the N assimilated by the crop prior to grain filling and of the prevailing growing season conditions (Masclaux-Daubresse et al., 2010). Several studies showed poor or no relationship between grain protein and VIs particularly with RNDVI (Aranguren et al., 2020; Dhillon et al., 2020; Wang et al., 2019). Magney et al. (2017) also found that RENDVI was the best predictor, explaining 81% of the variance in wheat N uptake. The red edge band is the transitional region between the visible red and NIR bands and is more sensitive to chlorophyll content and N concentrations in grain; therefore, it is more likely to reflect within-field spatial and temporal variations in N level during wheat development (Wang et al. 2019). This study showed that acquired high resolution orthomosaic imagery from sUAV based passive sensor gives researchers and growers enormous advantages for accurate and cost-effective measurements of wheat grain yield and protein content. Similar to Raun et al. (2005), these results also indicate that yield prediction equations for spring wheat can be established with only 2 years of field data acquired from a small portion of the field area. However, it is critical to validate these findings for the other part of region.

2.6. References

Aparicio, N., Villegas, D., Casadesus, J., Araus, J. L., & Royo, C. (2000). Spectral vegetation indices as nondestructive tools for determining durum wheat yield. *Agronomy Journal*, 92(1), 83-91.

Aranguren, M., Castellon, A., & Aizpurua, A. (2020). Crop Sensor Based Non-destructive Estimation of Nitrogen Nutritional Status, Yield, and Grain Protein Content in Wheat. Agriculture-Basel, 10(5).

Bean, G. M., Kitchen, N. R., Camberato, J. J., Ferguson, R. B., Fernandez, F. G., Franzen, D. W., . . . Shanahan, J. S. (2018). Active-Optical Reflectance Sensing Corn Algorithms Evaluated over the United States Midwest Corn Belt. *Agronomy Journal*, 110(6), 2552-210 2565.

Bendig, J., Yu, K., Aasen, H., Bolten, A., Bennertz, S., Broscheit, J., . . . Bareth, G. (2015). Combining UAV-based plant height from crop surface models, visible, and near infrared vegetation indices for biomass monitoring in barley. *International Journal of Applied Earth Observation and Geoinformation*, 39, 79-87.

Bushong, J. T., Miller, E. C., Mullock, J. L., Arnall, D. B., & Raun, W. R. (2016). Irrigated and rain-fed maize response to different nitrogen fertilizer application methods. *Journal of Plant Nutrition*, 39(13), 1874-1890.

Dhillon, J., Eickhoff, E., Aula, L., Omara, P., Weymeyer, G., Nambi, E., . . . Raun, W. (2020). Nitrogen management impact on winter wheat grain yield and estimated plant nitrogen loss. *Agronomy Journal*, 112(1), 564-577.

Erdle, K., Mistele, B., & Schmidhalter, U. (2011). Comparison of active and passive spectral sensors in discriminating biomass parameters and nitrogen status in wheat cultivars. *Field Crops Research*, 124(1), 74-84.

Fitzgerald, G. J. (2010). Characterizing vegetation indices derived from active and passive sensors. *International Journal of Remote Sensing*, 31(16), 4335-4348.

Goodwin, A. W., Lindsey, L. E., Harrison, S. K., & Paul, P. A. (2018). Estimating Wheat Yield with Normalized Difference Vegetation Index and Fractional Green Canopy Cover. *Crop Forage & Turfgrass Management*, 4(1).

Gozdowski, D., Stępień, M., Panek, E., Varghese, J., Bodecka, E., Rozbicki, J., & Samborski, S. (2020). Comparison of winter wheat NDVI data derived from Landsat 8 and active optical sensor at field scale. *Remote Sensing Applications: Society and Environment*, 20, 100409.

Guan, S. L., Fukami, K., Matsunaka, H., Okami, M., Tanaka, R., Nakano, H., . . . Takahashi, K. (2019). Assessing Correlation of High-Resolution NDVI with Fertilizer Application Level and Yield of Rice and Wheat Crops using Small UAVs. *Remote Sensing*, 11(2).

Krienke, B., Ferguson, R. B., Schlemmer, M., Holland, K., Marx, D., & Eskridge, K. (2017). Using an unmanned aerial vehicle to evaluate nitrogen variability and height effect with an active crop canopy sensor. *Precision Agriculture*, 18(6), 900-915.

Kyratzis, A. C., Skarlatos, D. P., Menexes, G. C., Vamvakousis, V. F., & Katsiotis, A. (2017). Assessment of Vegetation Indices Derived by UAV Imagery for Durum Wheat Phenotyping under a Water Limited and Heat Stressed Mediterranean Environment. *Frontiers in Plant Science*, 8.

Li, F., Miao, Y. X., Feng, G. H., Yuan, F., Yue, S. C., Gao, X. W., . . . Chen, X. P. (2014). Improving estimation of summer maize nitrogen status with red edge-based spectral vegetation indices. *Field Crops Research*, 157, 111-123.

Magney, T. S., Eitel, J. U. H., & Vierling, L. A. (2017). Mapping wheat nitrogen uptake from RapidEye vegetation indices. *Precision Agriculture*, 18(4), 429-451.

Maimaitijiang, M., Sagan, V., Sidike, P., Hartling, S., Esposito, F., & Fritschi, F. B. (2020). Soybean yield prediction from UAV using multimodal data fusion and deep learning. *Remote Sensing of Environment*, 237.

Marino, S., & Alvino, A. (2020). Agronomic Traits Analysis of Ten Winter Wheat Cultivars Clustered by UAV-Derived Vegetation Indices. *Remote Sensing*, 12(2).

Masclaux-Daubresse, C., Daniel-Vedele, F., Dechorgnat, J., Chardon, F., Gaufichon, L., & Suzuki, A. (2010). Nitrogen uptake, assimilation and remobilization in plants: challenges for sustainable and productive agriculture. *Annals of Botany*, 105(7), 1141-1157.

Naser, M. A., Khosla, R., Longchamps, L., & Dahal, S. (2020). Using NDVI to Differentiate Wheat Genotypes Productivity Under Dryland and Irrigated Conditions. *Remote Sensing*, 12(5).

Raun, W. R., Solie, J. B., Stone, M. L., Martin, K. L., Freeman, K. W., Mullen, R. W., . . . Johnson, G. V. (2005). Optical sensor-based algorithm for crop nitrogen fertilization. *Communications in Soil Science and Plant Analysis*, 36(19-20), 2759-2781.

Roberts, D. A., Roth, K. L., & Perroy, R. L. (2012). Hyperspectral Vegetation Indices. *Hyperspectral Remote Sensing of Vegetation*, 309-327.

Samborski, S. M., Tremblay, N., & Fallon, E. (2009). Strategies to Make Use of Plant Sensors Based Diagnostic Information for Nitrogen Recommendations. *Agronomy Journal*, 101(4), 800-816.

Schut, A. G. T., Traore, P. C. S., Blaes, X., & de By, R. A. (2018). Assessing yield and fertilizer response in heterogeneous smallholder fields with UAVs and satellites. *Field Crops Research*, 221, 98-107.

Sharma, L. K., Bu, H. G., Denton, A., & Franzen, D. W. (2015). Active-Optical Sensors Using Red NDVI Compared to Red Edge NDVI for Prediction of Corn Grain Yield in North Dakota, USA. *Sensors*, 15(11), 27832-27853.

Sripada, R. P., Heiniger, R. W., White, J. G., & Meijer, A. D. (2006). Aerial color infrared photography for determining early in-season nitrogen requirements in corn. *Agronomy Journal*, 98(4), 968-977.

Tubana, B., Harrell, D., Walker, T., Teboh, J., Lofton, J., Kanke, Y., & Phillips, S. (2011). Relationships of Spectral Vegetation Indices with Rice Biomass and Grain Yield at Different Sensor View Angles. *Agronomy Journal*, 103(5), 1405-1413.

Wang, K., Huggins, D. R., & Tao, H. Y. (2019). Rapid mapping of winter wheat yield, protein, and nitrogen uptake using remote and proximal sensing. *International Journal of Applied Earth Observation and Geoinformation*, 82.

Zhou, X., Zheng, H. B., Xu, X. Q., He, J. Y., Ge, X. K., Yao, X., . . . Tian, Y. C. (2017). Predicting grain yield in rice using multi-temporal vegetation indices from UAV-based multispectral and digital imagery. *Isprs Journal of Photogrammetry and Remote Sensing*, 130, 246-2.

APPENDIX

Table A1. Soil properties, fertilizer management, and date of planting and harvesting of sixteen spring wheat fields

Site	Texture	BD	pH	OM	Olsen-P	Available K	Fertilizer management	Planting Date	Harvesting Date
		Mg m^{-3}		g kg^{-1}	g kg^{-1}	g kg^{-1}			
2019									
Argyle, MN	Sandy clay loam	1.23	8.2	52	21	361	157 kg N ha^{-1} with N serve	Apr. 25	Jul. 30
Gentilly, MN	Sandy clay loam	1.39	7.1	51	18	242	Fall urea 145 kg N ha^{-1} and starter (12-40-0-10-1) at the rate112 kg ha^{-1}	May 9	Jul. 30
Dorothy, MN	Sandy loam	1.40	8.2	38	10	80	Fall anhydrous NH3 at 151 kg N ha^{-1}	May 15	Aug. 5
Mahnomen, MN	Sandy clay loam	1.31	7.1	57	19	159	Spring anhydrous NH_3 at 159 kg N ha^{-1} and 84 kg ha^{-1} of 11-52-0	May 10	Aug. 2
Ada, MN	Sandy clay loam	1.65	7.8	37	24	189	179 kg N ha^{-1}, 66 kg P2O5 ha^{-1}	May 14	Aug. 2
Red lake Falls, MN	Sandy loam	1.37	8.0	29	11	97	Fall 134 kg N ha^{-1}	May 10	Aug. 1
Thief River Falls, MN	Sandy loam	1.24	8.3	42	11	103	Spring 100 kg N ha^{-1}	May 9	Aug. 1
Rustad, MN	Sandy clay loam	1.17	7.8	57	20	278	Fall 123 kg N ha^{-1}	May 7	Jul. 31
2020									
Argyle, MN	Silty clay	1.05	8.3	53	3	279	364 kg N ha^{-1} urea (167 kg N ha-1) and 90 kg N ha^{-1} 11-52-0 ha^{-1} (10 kg N ha^{-1}	May 11	Aug.12
Gentilly, MN	Loam	1.25	8.3	20	6	67	336 kg urea ha^{-1} (155 kg N ha-1) 168 kg MESZ N (12-40-0-10-1) ha^{-1} (20 kg N ha^{-1})	May 12	Aug. 4

Table A1. Soil properties, fertilizer management, and date of planting and harvesting of sixteen spring wheat fields (continued)

Site	Texture	BD	pH	OM	Olsen-P	Available K	Fertilizer management	Planting Date	Harvesting Date
		Mg m^{-3}		g kg^{-1}	g kg^{-1}	g kg^{-1}			
Ada_GM, MN	Sandy loam	1.03	8.5	16	3	59	Spring 344 kg ha^{-1} urea and 56 kg ha^{-1} of 11-52-0 and 112 kg ha^{-1} of MOP	May 4	Aug. 4
Ada, MN	Sandy clay loam	0.99	8.6	31	7	95	Spring 291 kg ha^{-1} of urea and 90 kg ha^{-1} of 9-42-12	May 11	Aug. 12
Fosston, MN	Sandy clay loam	1.06	8.4	23	10	97	Spring 157 kg ha^{-1} of Anhydrous NH_3 and 44 kg ha^{-1} of 11-52-0	May 5	Aug. 12
Casselton, ND	Clay loam	1.11	7.7	51	4	289	N/A	N/A	Jul. 30
Rustad-no tile, MN	Sandy clay	1.14	8.3	30	8	181	190 kg N ha^{-1}, 56 kg P_2O_5 ha^{-1}, 11 kg K_2O ha^{-1} and 16 kg S ha^{-1}	Apr. 21	Jul. 28
Rustad-Tile, MN	Sandy clay loam	1.25	8.5	35	5	80	168 kg N, 45 kg P_2O_5 and 11 kg K_2O ha^{-1}	Apr. 25	Jul. 28

Table A2. Monthly rainfall (mm) and average air temperature (c) for the field sites used to collect active and passive remote sensing data, located across Minnesota and North Dakota during 2019 and 2020 growing seasons.

Site	Total Rainfall (mm)					Avg. Air Temp. (C)				
	April	May	June	July	August	April	May	June	July	August
					2019					
Ada	26(-10)	63(-20)	68(45)	103(10)	94(24)	5(-1)	11(-2)	18(0)	21(0)	18(-2)
Rustad	15(-26)	56(-24)	81(-24)	136(55)	70(2.6)	6(-1)	11(-3)	20(0)	22(0)	20(-3)
Mahnomen	30(-11)	50(-25)	66(-57)	94(6)	105(26)	5(-1)	10(-3)	19(1)	21(0)	18(-2)
Dorothy	37(11)	42(-26)	64(-25)	106(26)	111(38)	5(0)	11(-2)	19(1)	21(0)	18(-1)
Red Lake Falls	37(11)	42(-26)	64(-25)	106(26)	111(38)	5(0)	11(-2)	19(1)	21(0)	18(-1)
Gentilly	37(11)	42(-26)	64(-25)	106(26)	111(38)	5(0)	11(-2)	19(1)	21(0)	18(-1)
Thief River Falls	18(-14)	45(-31)	43(-71)	95(10)	59(-38)	4(-2)	10(-3)	18(0)	20(0)	17(-2)
Argyle	13(-12)	47(-23)	83(-11)	102(32)	119(42)	4(-2)	10(-2)	18(0)	20(0)	18(-2)
					2020					
Rustad (Tile)	40(-18)	80(-47)	85(-20)	154(73)	134(66)	4(-3)	12(-2)	21(2)	22(0)	20(-1)
Rustad (No Tile)	40(-18)	80(-47)	85(-20)	154(73)	134(66)	4(-3)	12(-2)	21(2)	22(0)	20(-1)
Casselton	39(5)	38(-34)	67(-32)	133(63)	122(57)	4(-3)	13(-1)	22(2)	23(2)	21(0)
Fosston	28(-12)	21(-54)	74(-48)	101(13)	163(84)	3(-3)	11(-2)	20(2)	22(1)	20(0)
Ada	22(-14)	34(-49)	57(-57)	103(10)	158(89)	3(-3)	12(-1)	21(2)	22(1)	20(-1)
Ada GM	22(-14)	34(-49)	57(-57)	103(10)	158(89)	3(-3)	12(-1)	21(2)	22(1)	20(-1)
Gentilly	12(-14)	33(-36)	100(12)	106(26)	78(5)	3(-3)	12(-1)	21(3)	22(2)	20(0)
Argyle	8.4(-17)	24(-45)	102(8)	112(42)	80(2)	2(-3)	11(-1)	19(1)	21(0)	19(0)

Table A3. Vegetation indices collected from passive (Micasense) and active sensors (RapidScan) at three different dates for sixteen wheat fields across Minnesota and North Dakota during 2019 and 2020 growing seasons

Site	Date	DAP	GDD	Rain	Stage	Active sensor		Passive sensor	
						RNDVI	RENDVI	RNDVI	RENDVI
					2019				
Rustad	18-Jun	54	711	67.6	8.2	0.82	0.37	0.88	0.48
	12-Jul	78	1208	241.7	>12	0.87	0.42	0.92	0.61
	22-Jul	88	1434	277.5	>12	0.75	0.29	0.88	0.54
TRF	19-Jun	41	583	42.4	6.6	0.71	0.32	0.83	0.42
	16-Jul	68	1131	149.7	>12	0.75	0.33	0.91	0.60
	23-Jul	75	1268	154.6	>12	0.69	0.28	0.87	0.54
RLF	19-Jun	40	576	42.4	6.5	0.76	0.34	0.87	0.47
	16-Jul	67	1123	149.7	>12	0.75	0.33	0.87	0.55
	22-Jul	73	1241	154.6	>12	0.69	0.28	0.83	0.49
Ada	18-Jun	35	525	93.8	5.9	0.78	0.32	0.86	0.53
	12-Jul	59	1001	206.1	11.8	0.83	0.38	0.93	0.61
	22-Jul	69	1221	219.3	>12	0.72	0.29	0.86	0.51
Mahnomen	19-Jun	40	596	70.1	6.7	0.78	0.32	0.87	0.40
	12-Jul	63	1059	174.3	>12	0.77	0.35	0.93	0.62
	22-Jul	73	1276	185.8	>12	0.79	0.34	0.91	0.59
Dorothy	26-Jun	42	631	123.8	7.2	0.86	0.39	0.91	0.49
	16-Jul	62	1050	210.4	>12	0.80	0.36	0.90	0.58
	23-Jul	69	1187	213.7	>12	0.74	0.31	0.88	0.54
Gentilly	26-Jun	48	754	98.3	8.7	0.85	0.38	0.91	0.50
	16-Jul	68	1178	190.1	>12	0.81	0.34	0.90	0.58
	23-Jul	75	1319	199.3	>12	0.75	0.28	0.86	0.46
Argyle	26-Jun	62	802	139.3	9.3	0.83	0.38	0.90	0.54
	16-Jul	82	1221	225.9	>12	0.74	0.34	0.90	0.61
	23-Jul	89	1358	229.2	>12	0.65	0.27	0.83	0.50
					2020				
Rus_Tile	5-Jun	41	557	35.3	6.3	0.54	0.23	0.70	0.33
	19-Jun	55	854	97.8	10	0.76	0.33	0.89	0.54
	10-Jul	76	1324	178.6	>12	0.67	0.26	0.80	0.43
Rus_NT	5-Jun	45	601	36.1	6.8	0.82	0.34	0.89	0.46
	19-Jun	59	898	98.6	10.5	0.79	0.36	0.91	0.60
	10-Jul	80	1368	179.4	>12	0.53	0.20	0.65	0.31
Casselton	5-Jun	38	523	38.9	5.8	0.69	0.27	0.73	0.31
	19-Jun	52	828	88.5	9.7	0.81	0.34	0.90	0.50
	10-Jul	73	1312	144.3	>12	0.72	0.30	0.80	0.45

Table A3. Vegetation indices collected from passive (Micasense) and active sensors (RapidScan) at three different dates for sixteen wheat fields across Minnesota and North Dakota during 2019 and 2020 growing seasons (continued)

Site	Date	DAP	GDD	Rain	Stage	Active sensor		Passive sensor	
						RNDVI	RENDVI	RNDVI	RENDVI
Ada	11-Jun	31	508	51.6	5.6	0.71	0.30	0.74	0.35
	24-Jun	44	768	60.2	8.9	0.82	0.36	0.91	0.56
	15-Jul	65	1257	99.1	>12	0.73	0.32	0.84	0.53
Ada GM	11-Jun	38	554	70.4	6.2	0.83	0.33	0.86	0.42
	24-Jun	51	814	79	9.5	0.87	0.39	0.92	0.58
	15-Jul	72	1304	117.9	>12	0.68	0.27	0.83	0.48
Fosston	11-Jun	37	524	70.6	5.8	0.81	0.30	0.84	0.36
	24-Jun	50	772	86.6	9	0.86	0.38	0.92	0.56
	15-Jul	71	1244	116.6	>12	0.72	0.27	0.83	0.48
Gentilly	12-Jun	31	508	30.7	5.6	0.50	0.18	0.46	0.19
	22-Jun	41	711	54.1	8.2	0.76	0.28	0.68	0.31
	16-Jul	65	1258	164.4	>12	0.57	0.23	0.72	0.41
Argyle	12-Jun	31	474	63.8	5.2	0.58	0.20	0.66	0.24
	22-Jun	41	660	73.9	7.6	0.83	0.34	0.88	0.47
	16-Jul	65	1163	172.1	>12	0.77	0.33	0.92	0.60